

Article

**Structure, Activity, and Stability of Triphenyl
Phosphine-Modified Rh/SBA-15 Catalyst for Hydroformylation
of Propene: A High-Resolution Solid-State NMR Study**

Xijie Lan, Weiping Zhang, Li Yan, Yunjie Ding, Xiuwen Han, Liwu Lin, and Xinhe Bao

J. Phys. Chem. C, **2009**, 113 (16), 6589-6595 • Publication Date (Web): 30 March 2009

Downloaded from <http://pubs.acs.org> on April 17, 2009

More About This Article

Additional resources and features associated with this article are available within the HTML version:

- Supporting Information
- Access to high resolution figures
- Links to articles and content related to this article
- Copyright permission to reproduce figures and/or text from this article

[View the Full Text HTML](#)



ACS Publications
High quality. High impact.

Structure, Activity, and Stability of Triphenyl Phosphine-Modified Rh/SBA-15 Catalyst for Hydroformylation of Propene: A High-Resolution Solid-State NMR Study

Xijie Lan, Weiping Zhang,* Li Yan, Yunjie Ding, Xiuwen Han, Liwu Lin, and Xinhe Bao*

State Key Laboratory of Catalysis, Dalian Institute of Chemical Physics, Chinese Academy of Sciences, 457 Zhongshan Road, Dalian 116023, China

Received: November 27, 2008; Revised Manuscript Received: February 26, 2009

A ligand (triphenyl phosphine, PPh₃)-modified heterogeneous PPh₃-Rh(CO)/SBA-15 catalyst and supported Wilkinson complex HRh(CO)(PPh₃)₃/SBA-15 catalyst were prepared and examined in the hydroformylation of propene. Heterogeneous PPh₃-Rh(CO)/SBA-15 catalyst showed much higher activity and stability in this reaction. Multinuclear ¹H, ²⁹Si, ³¹P, and ¹⁷O MAS NMR and two-dimensional ¹⁷O MQ MAS NMR together with XRD and N₂ adsorption were employed to study the local structures of these two catalysts. Quantitative ¹H and ²⁹Si MAS NMR and qualitative one- and two-dimensional ¹⁷O MAS and MQ MAS NMR indicate that in the presence of CO the silanols on the surface of SBA-15 can react with rhodium carbonyls to form the Si-O-Rh bonds at the interface between the catalyst and the support. ³¹P MAS NMR spectra demonstrate a similar Wilkinson complex structure is produced on the heterogeneous PPh₃-Rh(CO)/SBA-15 catalyst. The formation of Si-O-Rh bonds at the interface may immobilize the Rh complex during the long reaction. These may be correlated to the higher performances of heterogeneous PPh₃-Rh(CO)/SBA-15 catalyst in propene hydroformylation.

1. Introduction

Hydroformylation involves the reaction of carbon monoxide and hydrogen with an alkene to produce aldehydes, which is one of the oldest homogeneous catalytic reactions.^{1,2} The commonly used catalyst for this reaction is based on Rh complex due to its high activity and selectivity at milder reaction conditions.³ However, the practical applications have been limited by difficulties in achieving industrially viable catalyst-product separation.⁴ To solve this problem, many approaches have been explored, which can broadly be grouped into two types. One is biphasic system using aqueous biphasic, supercritical fluids, ionic liquids, or supported ionic liquid phase catalyst.⁵⁻⁷ The other is often used to anchor the catalyst on the polymer resin or silica.⁸⁻¹¹ However, low activity, selectivity, and stability of these catalysts may hamper their actual application in the chemical industry. Recently, our laboratory reported that heterogeneous catalyst Rh/SiO₂ modified by triphenyl phosphine (PPh₃) showed higher selectivity and stability for propylene hydroformylation than the supported Wilkinson catalyst HRh(CO)(PPh₃)₃/SiO₂.¹² The heterogeneous catalyst need not be separated from the product after reaction and has almost no Rh leaching, yet the catalyst structure and its correlation to performance remain unclear. Multinuclear solid-state NMR is a powerful tool in the characterization of the local structures of zeolites and other solid catalysts.¹³ ¹H, ²⁹Si, and ²⁷Al MAS NMR techniques are routinely carried out on porous materials and have contributed significantly to the understanding of the structure and properties of these materials. Oxygen atoms constitute a major part of the framework and it is via the oxygen atoms that many adsorbed species and anchored catalysts are bound to the zeolite framework. However, little work has been performed in ¹⁷O MAS NMR because of both the low natural abundance of the NMR-activity nucleus (only 0.037%) and the broad ¹⁷O

resonance typically observed for the framework sites caused largely by the second-order quadrupolar interaction. ¹⁷O MAS NMR should, in principle, provide valuable information on the local structure because it is a quadrupolar nucleus with $I = 5/2$, which is sensitive to the surrounding electric field gradient.¹⁴ Although the nature abundance is low, it is possible to enrich the sample with either ¹⁷O containing gas or water.^{14,15} The multiple-quantum magic angle spinning (MQ MAS) NMR can be used to remove the second-order quadrupolar interaction. This method produces two-dimensional spectra with an isotropic dimension, which is free of the second-order quadrupolar interaction, and an anisotropic dimension which contains the second-order quadrupolar line shapes.¹⁶ In this study, multinuclear MAS NMR has been used to elucidate the local structures of the heterogeneous PPh₃-Rh(CO)/SBA-15 and supported Wilkinson complex HRh(CO)(PPh₃)₃/SBA-15 catalysts. This includes the less routine one-dimensional ¹⁷O MAS and two-dimensional multiple-quantum (MQ) MAS NMR to illustrate the variations of the framework structures of the support. ²⁹Si, ¹H, and ³¹P MAS NMR are carried out to understand the interaction of different hydroxyls on the support with the rhodium species and the subsequent coordination of PPh₃. When these are combined with other techniques such as XRD and N₂ adsorption, the structure differences of these two types of catalysts have been revealed, which can be correlated to the higher activity and stability of heterogeneous PPh₃-Rh(CO)/SBA-15 catalyst in propene hydroformylation.

2. Experimental Section

2.1. Catalyst Preparation. The natural abundance of ¹⁷O is only 0.037%. To carry out the ¹⁷O MAS NMR experiments, the ¹⁷O enriched SBA-15 support (pore diameter of ca. 6.0 nm from Jilin University High Tech. Co. Ltd.) was prepared by heating the dehydrated sample in ¹⁷O₂ gas (50% enriched ¹⁷O₂, Isotec Inc.) at atmospheric pressure at 853 K for 12 h.¹⁵ Catalysts PPh₃-*n*Rh(CO)/SBA-15 with *n* denoting 1.0 and 5.0 wt % of

* Authors to whom correspondence should be addressed. Fax: +86-411-8469 4447. E-mail: wpzhang@dicp.ac.cn (W.Z.); xhbao@dicp.ac.cn (X.B.).

Rh were prepared according to our previous procedures.¹² In general, the support SBA-15 was impregnated with an aqueous solution of rhodium chloride (Shanghai July Chemical Co. Ltd.) using the incipient wetness method. After that, samples were dried at 373 K first, then calcined at 673 K in a quartz tube, and finally reduced by H₂ at 673 K. The obtained precursors were introduced into the PPh₃ solution in toluene and stirred for 0.5 h, then the solvent was removed under vacuum, and the resultant samples with the molar ratio of P/Rh = 4:1 were stored in an argon atmosphere. The samples were reduced by H₂ at 393 K for 1 h and then purged with CO for 1 h to get the resultant PPh₃-*n*Rh(CO)/SBA-15 catalysts. The Wilkinson complex HRh(CO)(PPh₃)₃ was synthesized as that reported in the reference.¹⁷ It was then impregnated on SBA-15 using the incipient wetness method to obtain supported Wilkinson complex HRh(CO)(PPh₃)₃/SBA-15 with ca. 1.0 wt % Rh. All these experiments were carried out under the protection of argon. The metal dispersion was determined by hydrogen chemisorption at 323 K on Shimadzu Instrument. The value for the rhodium dispersion was calculated to be 0.51 on heterogeneous 1Rh/SBA-15 catalyst by assuming a stoichiometry (H:Rh) of 1:1.

2.2. Catalytic Evaluation. The propene hydroformylation was conducted in a continuous flow fixed-bed reactor (i.d. 6.0 mm) at 403 K and 1.0 MPa of 1:1:1 molar ratio of CO/H₂/CH₂=CHCH₃. Before the reaction, the catalysts (~0.2 g) were purged in N₂ at 393 K for 2 h and then switched to the reactant gases. The effluent was passed through a condenser filled with 100 mL of cold deionized water. The butyraldehyde hydroformylation products were captured completely by dissolution into the water in the condenser and analyzed by an HP-7890N GC with an HP-INNOWAX column, using an FID detector and ethanol as an internal standard. The tail gas was analyzed by an online HP-6890N GC with a Poropak-QS column and a TCD detector. The yield of butyraldehyde was calculated in terms of the amount of butyraldehyde obtained in 1 h on a mole of dispersed Rh metal.

2.3. XRD and BET Measurements. Low-angle X-ray diffraction patterns were obtained at room temperature on a Rigaku D/Max-RB diffractometer using Cu K α radiation. Powder diffractograms of the samples were recorded over a range of 2 θ values from 0.5° to 10° under the conditions of 40 kV and 50 mA at a scanning rate of 0.5° per minute. The nitrogen adsorption experiments were performed at 77 K on an ASAP 2000 system. The samples were outgassed at 473 K for 10 h before the measurements.

2.4. MAS NMR Measurements. All MAS NMR experiments were carried out on a Varian Infinityplus-400 spectrometer. ²⁹Si MAS and CP/MAS NMR spectra were recorded at 79.4 MHz with the samples spun at 4 kHz using a 7.5 mm probe head. ²⁹Si MAS NMR spectra with high-power proton decoupling were acquired with $\pi/4$ pulse width of 1.9 μ s, 360 s recycle delay, and 120 scans. ¹H \rightarrow ²⁹Si CP/MAS NMR spectra were recorded with a 4 s recycle delay, 1024 scans, and contact time of 1.0 ms. ¹H MAS NMR spectra were collected using a 4 mm probe head. Before the ¹H MAS NMR experiments, samples were dehydrated at 473 K and a pressure below 10⁻² Pa for 20 h. ¹H MAS NMR spectra were collected at 399.9 MHz with the samples spun at 10 kHz, $\pi/4$ pulse width of 1.3 μ s, 4.0 s recycle delay, and 200 scans. To obtain quantitative results, all samples were weighed and the spectra were calibrated by measuring a known amount of 1,1,1,3,3,3-hexafluoro-2-propanol under the same conditions.¹⁸ Chemical shifts of the ²⁹Si and ¹H MAS NMR spectra were referenced to 4,4-dimethyl-4-silapentane sulfonate sodium (DSS) at 0 ppm. ³¹P MAS NMR spectra

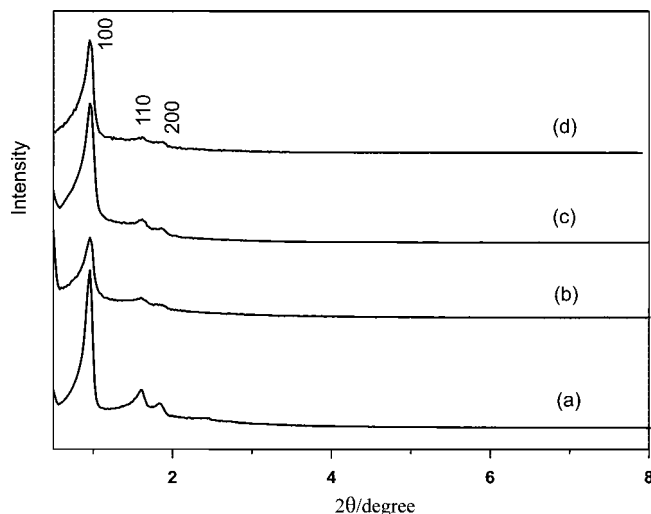


Figure 1. Small-angle XRD patterns of (a) SBA-15, (b) HRh(CO)(PPh₃)₃/SBA-15, (c) PPh₃-1Rh(CO)/SBA-15, and (d) PPh₃-5Rh(CO)/SBA-15.

were recorded at 161.8 MHz using a 2.5 mm probe head with the samples spun at 25 kHz, $\pi/4$ pulse width of 0.95 μ s, 3 s recycle delay, and 2048 scans. The chemical shifts were referenced to 85% H₃PO₄. ¹⁷O MAS and MQ MAS NMR spectra were collected using a 4 mm probe head at 54.2 MHz with the samples spun at 15 kHz. ¹⁷O MAS NMR spectra were collected using a $\pi/4$ pulse width of 0.9 μ s, 8.0 s recycle delay, and 30000 scans and the chemical shift was referenced to water. The deconvolution of the spectra was conducted using dmfit software.¹⁹ The error for the deconvolution could be estimated at about $\pm 2\%$. Two-dimensional ¹⁷O triple quantum (3Q) MAS NMR spectra were collected with modified fast amplitude modulation (FAM) shifted echo pulse sequences comprising two hard pulses of duration 5.1 and 1.8 μ s and a selective pulse with duration of 24.0 μ s.²⁰ The values of the quadrupolar product (P_Q) and the isotropic chemical shift (δ_{iso}) for each oxygen species may be obtained from the δ_{F1} and δ_{F2} positions (in ppm) of the center of gravity of each two-dimensional ridge line shape. For $I = 5/2$ nuclei these parameters are given by²¹

$$\delta_{iso} = (17\delta_{F1} + 10\delta_{F2})/27 \quad (1)$$

$$P_Q = QCC\sqrt{1 + \eta^2/3} = \left(\frac{17}{162000}\gamma_L^2(\delta_{F1} - \delta_{F2})\right)^{1/2} \quad (2)$$

where δ_{F1} and δ_{F2} are the center of gravity of the resonance in the isotropic (F_1) dimension and in the anisotropic (F_2) dimension, respectively, and γ_L , QCC, and η are the Larmor frequency, the quadrupolar coupling constant, and the asymmetry parameter, respectively.

3. Results and Discussion

3.1. XRD Patterns and N₂ Adsorption Data. Figure 1 shows the low-angle XRD patterns of the samples. It can be seen that all patterns have three reflection peaks that can be indexed to the (100), (110), and (200) diffraction lines characteristic of the hexagonal structure. The ordered mesostructure of SBA-15 support is maintained after loading PPh₃-Rh(CO) or Wilkinson complex HRh(CO)(PPh₃)₃. The intensities of three reflections gradually decrease with loading of the Rh complexes,

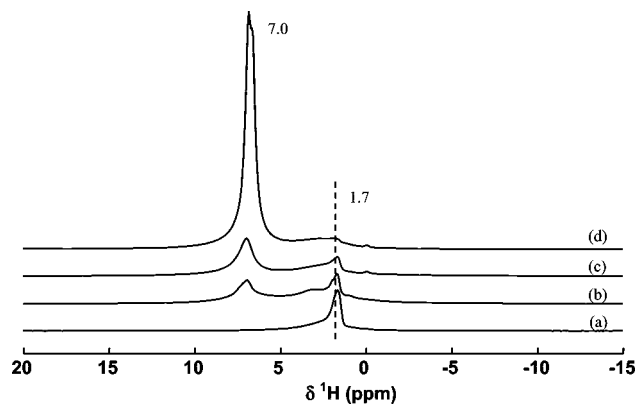


Figure 2. ^1H MAS NMR spectra of (a) SBA-15, (b) $\text{HRh}(\text{CO})(\text{PPh}_3)_3/\text{SBA-15}$, (c) $\text{PPh}_3\text{-1Rh}(\text{CO})/\text{SBA-15}$, and (d) $\text{PPh}_3\text{-5Rh}(\text{CO})/\text{SBA-15}$.

which indicate pore filling of the host SBA-15 support because pore filling can reduce the scattering contrast between the pores and the walls of the mesoporous material.^{22,23}

Table 1 lists the BET surface areas of the samples, which are calculated from the N_2 physisorption isotherms. The surface area of SBA-15 decreases obviously after loading the rhodium complex. For example, loading of 5 wt % Rh species on SBA-15 support leads to ca. 50% reduction in the BET surface area. This also indicates the inclusion of Rh complexes into the channels of SBA-15, and interactions may occur between the rhodium species and the SBA-15 support.

3.2. ^1H MAS NMR. High-resolution ^1H MAS NMR is a useful and direct method for characterizing the hydroxyls in porous materials. Compared with IR, it can provide quantitative information on the interaction between the metal ions and the hydroxyl species on the support without the difficulties of extinction coefficients.²⁴ The ^1H MAS NMR spectra of the catalysts are shown in Figure 2. ^1H MAS NMR spectrum of SBA-15 exhibits two hydroxyl groupings, i.e., single and hydrogen-bonded silanols at 1.7 and 2.4 ppm, respectively.²³ Two new resonance peaks at about 3.2 and 7.0 ppm can be seen after loading heterogeneous catalyst $\text{PPh}_3\text{-Rh}(\text{CO})$ or impregnating Wilkinson catalyst. The newly resonance peak at 7.0 ppm is assigned to PPh_3 , and the peak at about 3.2 ppm can be attributed to the physisorbed water or spillover hydrogen.²⁵ The signal of Rh-H species is not observed in the spectrum of supported Wilkinson complex $\text{HRh}(\text{CO})(\text{PPh}_3)_3/\text{SBA-15}$ catalyst, which is expected to appear at around -10 ppm.²⁶ This may be due to the reaction of $\text{HRh}(\text{CO})(\text{PPh}_3)_3$ with the silanols on the support or self-condensation to form dimeric species.²⁷ After quantification, the total amount of hydroxyls on SBA-15 is about 2.0 mmol g^{-1} after calibration by the external standard. The amount of single silanol at 1.7 ppm decreases more readily from 1.1 to 0.39 mmol g^{-1} when loading heterogeneous catalyst $\text{PPh}_3\text{-5Rh}(\text{CO})$, while there is no obvious change after impregnating Wilkinson complex catalyst $\text{HRh}(\text{CO})(\text{PPh}_3)_3$ (see Table 1). This indicates that the silanols on SBA-15 may react with the rhodium species, which may be in favor of the immobilization of heterogeneous $\text{PPh}_3\text{-Rh}(\text{CO})$ complex on SBA-15 support.

3.3. ^{29}Si MAS and $^1\text{H}\text{-}^{29}\text{Si}$ CP/MAS NMR. Figure 3 displays the ^{29}Si MAS NMR spectra of the samples. For support SBA-15 (Figure 3a), there are three resonance peaks at -93.8 , -102.5 , and -111.5 ppm, which can be assigned to Q^2 [$\text{Si}(\text{OSi})_2(\text{OH})_2$], Q^3 [$\text{Si}(\text{OSi})_3\text{OH}$], and Q^4 [$\text{Si}(\text{OSi})_4$], respectively.^{23,28} The corresponding $^1\text{H}\text{-}^{29}\text{Si}$ CP/MAS NMR spectrum of SBA-

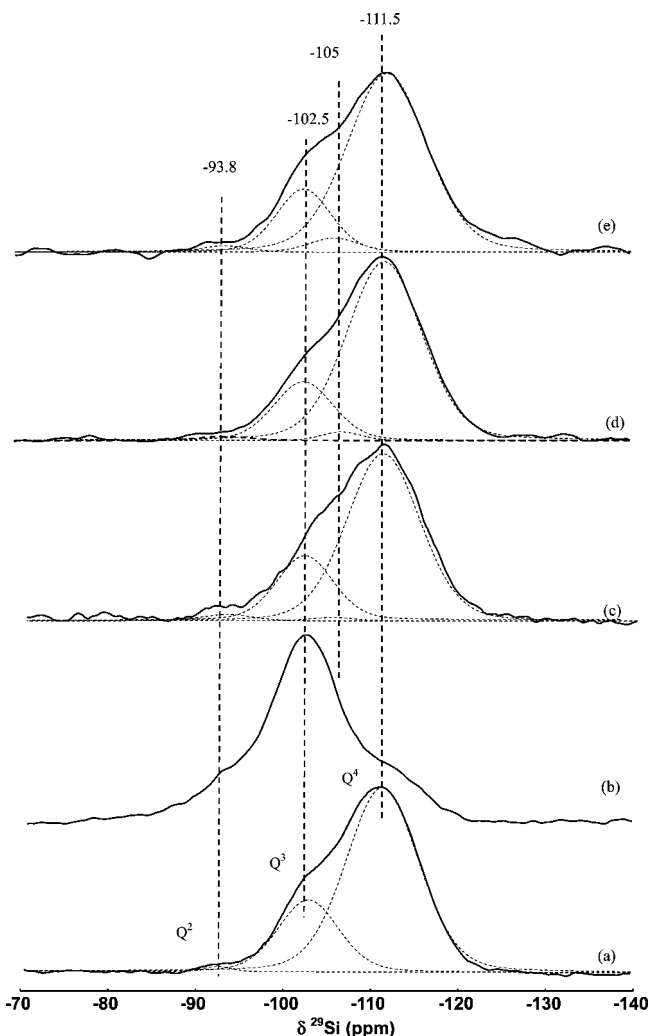


Figure 3. ^{29}Si MAS NMR spectra of (a) SBA-15, (c) $\text{HRh}(\text{CO})(\text{PPh}_3)_3/\text{SBA-15}$, (d) $\text{PPh}_3\text{-1Rh}(\text{CO})/\text{SBA-15}$, (e) $\text{PPh}_3\text{-5Rh}(\text{CO})/\text{SBA-15}$; (b) ^{29}Si CP/MAS NMR spectra of SBA-15.

15 is shown in Figure 3b. After cross-polarization, the intensity of the peaks at ca. -102.5 and -93.8 ppm shows a great increase, which indicates that these signals should be related to the species coupling strongly with the hydroxyl protons. This further confirms that the signals at -102.5 and -93.8 ppm in ^{29}Si MAS NMR spectra should be assigned to the Q^3 and Q^2 silanols, respectively. After heterogeneous catalyst $\text{PPh}_3\text{-Rh}(\text{CO})$ is loaded, a new resonance peak centered at ca. -105 ppm is observed after deconvolution of the spectra. This peak may be assigned to the [$\text{Si}(\text{OSi})_3\text{ORh}$] species in terms of the chemical shift range,²⁹ which may come from the interaction between the support SBA-15 and the rhodium species as shown by the above ^1H MAS NMR measurements. However, for the supported Wilkinson complex catalyst $\text{HRh}(\text{CO})(\text{PPh}_3)_3$, this peak is relatively weak. The concentration of all kinds of Si species in the samples can be determined from the corresponding deconvoluted ^{29}Si MAS NMR spectra and the results are listed in Table 1. It is found that the concentration of [$\text{Si}(\text{OSi})_3\text{ORh}$] in the samples increases to 3.4% when Rh increases to 5%; meanwhile, the concentration of silanols, e.g., Q^3 species, decreases correspondingly. However, only 0.4% of [$\text{Si}(\text{OSi})_3\text{ORh}$] species is formed on the supported Wilkinson complex $\text{HRh}(\text{CO})(\text{PPh}_3)_3/\text{SBA-15}$ catalyst, which is less than that on the heterogeneous $\text{PPh}_3\text{-Rh}(\text{CO})/\text{SBA-15}$ catalyst at the

TABLE 1: BET Surface Areas, Silanol Concentrations, and the Silicon Species Percentage of the Catalysts

sample	SBA-15	HRh(CO)(PPh ₃) ₃ / SBA-15	PPh ₃ -1Rh(CO)/ SBA-15	PPh ₃ -5Rh(CO)/ SBA-15
BET surface area (m ² /g of support)	702	503	370	243
single silanol concentration from ¹ H MAS NMR (mmol/g of support)	1.1	1.09	0.52	0.39
Q ³ species content from ²⁹ Si MAS NMR (%)	24.4	22.8	20.0	18.6
[Si-O-Rh] species content from ²⁹ Si MAS NMR (%)	N/A	0.4	1.9	3.4

same Rh loading. From quantitative ²⁹Si MAS NMR measurements, it is also known that Rh species interact with silanols on the support to form Si-O-Rh species, and such species can be produced more readily on the heterogeneous PPh₃-Rh(CO)/SBA-15 catalyst.

3.4. One-Dimensional ¹⁷O MAS and Two-Dimensional ¹⁷O MQ MAS NMR. In metal silicate gels the formation of M-O-Si bonds can be clearly detected by ¹⁷O NMR and makes structural modeling much less ambiguous than that based on ²⁹Si MAS NMR alone.³⁰ The ¹⁷O MAS NMR experiments were conducted to further confirm the existence of Si-O-Rh species. The one-pulse ¹⁷O MAS NMR spectra of the samples are shown in the Supporting Information. As demonstrated, each spectrum has a broad resonance signal centered at around 0 ppm, which is the characteristic second-order quadrupolar line shape coming from several overlapped components. After the catalysts are loaded, the one-dimensional ¹⁷O MAS NMR spectra are similar with little indication of different distinct oxygens in the samples. To resolve these overlapped oxygen species, the two-dimensional (2D) MQ MAS technique is used to remove fully the second-order quadrupolar broadening, but it does reflect distributions in QCC and δ_{iso} . In the 2D 3Q MAS NMR spectrum the projection onto the F₂ axis yields a conventional MAS spectrum, still showing the characteristic feature of second-order quadrupolar broadening but distorted by the three-quantum excitation. The high-resolution spectrum obtained in the projection onto the F₁ axis consists of isotropic peaks free of anisotropic second-order quadrupolar broadening. The 2D ¹⁷O MQ MAS NMR spectra of ¹⁷O-enriched SBA-15 and their F₁/F₂ projections are shown in Figure 4a. Similar to the one-dimensional ¹⁷O MAS NMR spectrum, the anisotropic projection of ¹⁷O MQ MAS NMR spectrum of SBA-15 shows two broad signals centered at $\delta_{\text{F}_2} = -5.6$ and -33.9 ppm, respectively. The isotropic projection, however, shows a relatively narrow resonance with a maximum at $\delta_{\text{F}_1} = 77.6$ ppm and a shoulder centered at $\delta_{\text{F}_1} = 70.3$ ppm, which may be assigned to Si-O-Si and Si-O-H species, respectively. According to eqs 1 and 2, we can extract the NMR parameters for these two species; e.g., the Si-O-Si species have the isotropic chemical shift (δ_{iso}) of 46.8 ppm and large quadrupolar constant (P_Q) of 5.0 MHz, whereas the Si-O-H species have the δ_{iso} of 31.7 ppm and P_Q of 5.7 MHz. This is consistent with the previous results; i.e., silanol hydroxyls experience larger quadrupolar constant than Si-O-Si species.³¹ To obtain a better ¹⁷O MQ MAS NMR spectrum, only the sample without PPh₃ but with high Rh loading and reacted with CO was used to compare with the support. Figure 4b shows the ¹⁷O MQ MAS NMR spectrum of the sample with 5 wt % Rh loading on the ¹⁷O-enriched SBA-15. A new resonance peak at $\delta_{\text{F}_2} = -23.8$ ppm and $\delta_{\text{F}_1} = 77.0$ ppm appears clearly between the Si-O-Si and Si-O-H species in this sample. This new signal has δ_{iso} of 39.6 ppm and P_Q of 5.6 MHz. Meanwhile, the isotropic chemical shifts of Si-O-Si and Si-O-H species and their quadrupolar constants have almost no big variations. This new signal can be assigned to Si-O-Rh species in terms of the isotropic chemical shift.^{32,33} Consequently, after the rhodium complex is

treated by CO, the ¹⁷O MQ MAS NMR spectrum in the isotropic dimension clearly demonstrates the formation of Si-O-Rh bonds on the surface of SBA-15 support. This further confirms the results from ²⁹Si MAS NMR experiments.

3.5. ³¹P MAS NMR. Figure 5 shows the ³¹P MAS NMR spectra of the samples. There is only a broad line centered at ca. 35.2 ppm in the spectrum of supported Wilkinson complex HRh(CO)(PPh₃)₃/SBA-15 catalyst, which could be attributed to the PPh₃ coordinated to the Rh of the Wilkinson complex.³⁴ There are two signals in the spectra of the heterogeneous PPh₃Rh/SBA-15 catalysts: one narrow peak at -5.5 ppm is ascribed to the free PPh₃ which has no coordination with the Rh,¹² and a broad signal centered at ca. 36.8 ppm could be assigned to PPh₃ coordinated to the surface of Rh particles by comparing the chemical shift of PPh₃ in the supported Wilkinson complex HRh(CO)(PPh₃)₃/SBA-15 catalyst. A very small chemical shift difference may be due to the change of electronic state of Rh species in these two systems. The amount of free PPh₃ in the heterogeneous catalyst with 1 wt % Rh is about 61% as estimated from the ³¹P MAS NMR spectrum. The P/Rh molar ratio on the external surface of Rh metal particles could be ca. 3.0 if the Rh dispersion of 0.51 and starting P/Rh ratio of 4.0 are considered. Figure 5 indicates that PPh₃ can be chemically adsorbed on the surface of heterogeneous Rh/SBA-15 catalyst, which is similar to the coordination structure of PPh₃ in supported Wilkinson complex.

3.6. Catalytic Performance of PPh₃-Rh/SBA-15 and HRh(CO)(PPh₃)₃/SBA-15 for Hydroformylation of Propene. The catalytic performances of PPh₃-Rh(CO)/SBA-15 and HRh(CO)(PPh₃)₃/SBA-15 with 1.0 wt % Rh for propene hydroformylation are shown in Figure 6. It is obvious that PPh₃-Rh/SBA-15 exhibits higher activity and stability than HRh(CO)(PPh₃)₃/SBA-15 for this reaction during the time on stream of 50 h. The turnover frequency (TOF) can reach about 175 h⁻¹ after the run of 30 h and remain stable up to 50 h on the heterogeneous PPh₃-Rh/SBA-15 catalyst, whereas the highest TOF is around 60 h⁻¹ on the supported Wilkinson complex HRh(CO)(PPh₃)₃/SBA-15 catalyst, and the activity decreases obviously after the run of 10 h. The selectivities of butyraldehyde for both catalysts are ca. 98%. However, the molar ratio of *n*-butyraldehyde to *iso*-butyraldehyde (*n/i* ratio) in the product of heterogeneous PPh₃-Rh/SBA-15 catalyst can be up to 7.0, which is higher than that of the supported Wilkinson complex HRh(CO)(PPh₃)₃/SBA-15 catalyst during the entire run.

For preparation of heterogeneous PPh₃-Rh(CO)/SBA-15 catalyst, RhCl₃/SBA-15 was reduced by H₂, and the metallic Rh was formed on the support as revealed by the XPS measurements in our previous study.¹² After adsorption of PPh₃ and further treatment by syngas, the ligands can be chemically adsorbed on the external surface of rhodium to form the PPh₃-Rh(CO) complex, which is similar to the coordination structure in the HRh(CO)(PPh₃)₃ Wilkinson complex as evidenced by ³¹P MAS NMR spectra. Our previous results show that in this case the state of Rh on its external surface is Rh^{δ+} ($0 < \delta < 1$), whereas in the bulk it is still metallic.¹² As

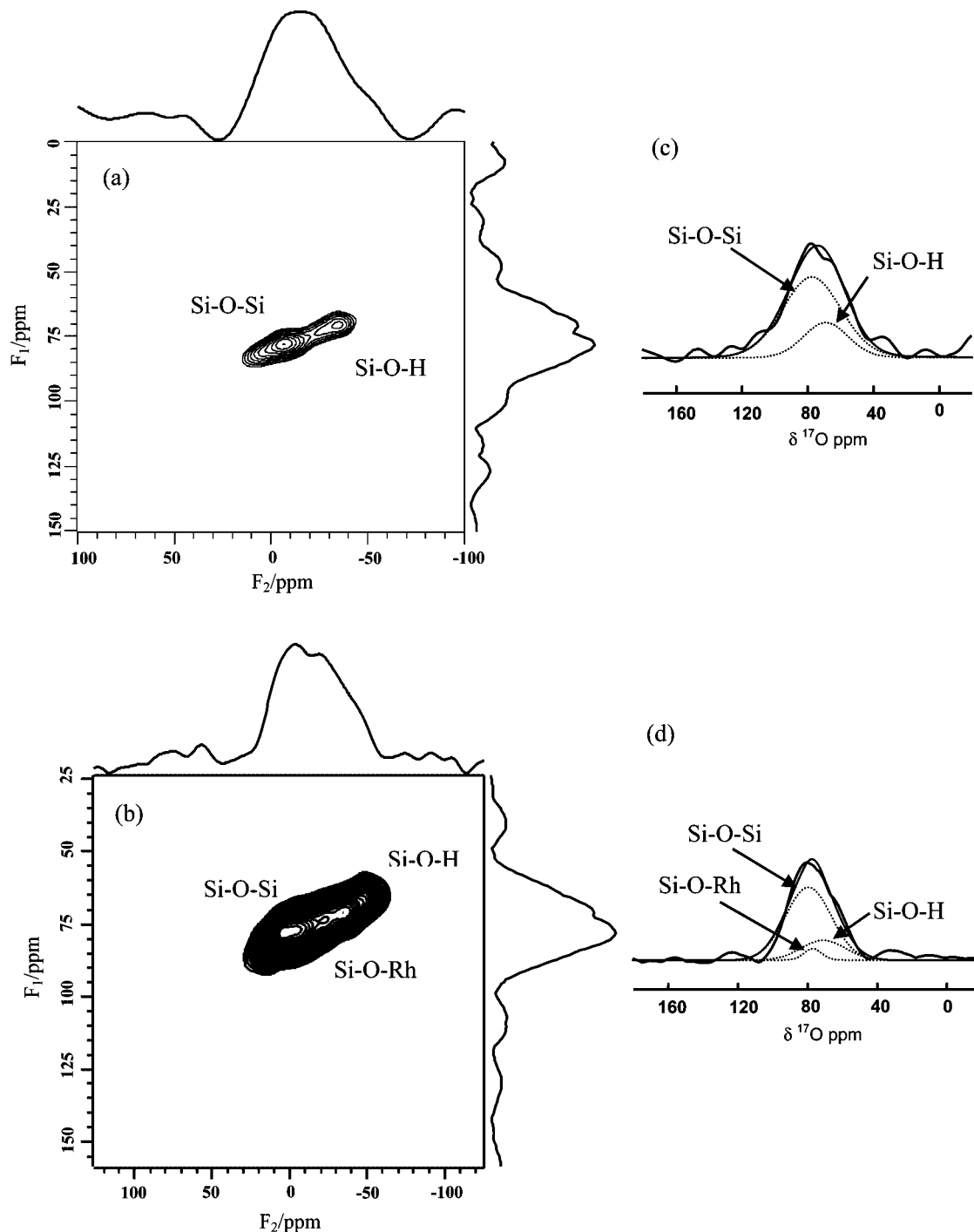


Figure 4. Two-dimensional ^{17}O MQ MAS NMR spectra of (a) SBA-15, (b) 5Rh(CO)/SBA-15, and their corresponding fitting results of the isotropic projection (c) and (d).

demonstrated by Prins and co-workers³⁵ and Iwasawa and co-workers³⁶ in their study of the Rh/Al₂O₃ catalyst by EXAFS and XPS in the presence of syngas, the surface hydroxyl groups (Al-OH) can react with Rh(CO)_n to form the Al-O-Rh(CO) species. This is similar in our case. The silanols on the SBA-15 support may also react with rhodium carbonyls to obtain the Si-O-Rh(CO) species at the interface between the catalyst and the support, which are confirmed by the above ^{29}Si MAS NMR as well as one- and two-dimensional ^{17}O MQ MAS NMR investigations. So the PPh₃-Rh(CO) complex can be tightly grafted on the support SBA-15 through the Si-O-Rh bonds at the interface between the catalyst and the support, whereas

for the supported Wilkinson complex HRh(CO)(PPh₃)₃/SBA-15 catalyst, such species are quite small. Combined with catalytic performance data, it can be deduced that there are similar Wilkinson complex structures in the heterogeneous PPh₃-Rh(CO)/SBA-15 catalyst. The formation of Si-O-Rh bonds at the interface between the catalyst and the support may immobilize the rhodium complex during the long reaction. These may account for the higher activity and stability of heterogeneous PPh₃-Rh(CO)/SBA-15 catalyst in propene hydroformylation. The higher *n/i* ratio of butyraldehyde on heterogeneous catalyst may be due to the higher P/Rh molar ratio on the external surface of Rh metal particles when taking the Rh

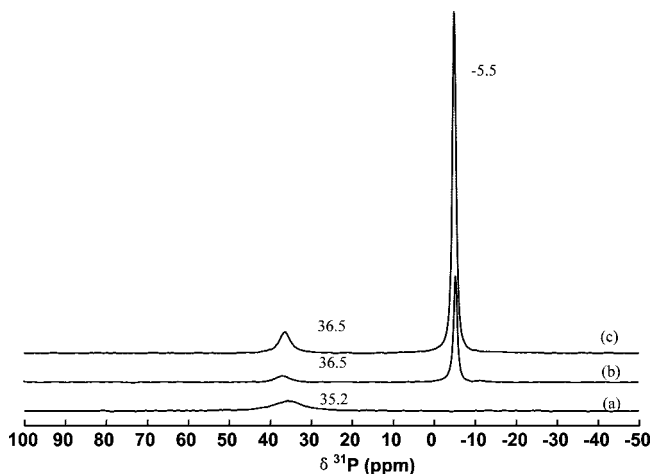


Figure 5. ^{31}P MAS NMR spectra of (a) $\text{HRh}(\text{CO})(\text{PPh}_3)_3/\text{SBA-15}$, (b) $\text{PPh}_3\text{-1Rh}(\text{CO})/\text{SBA-15}$, and (c) $\text{PPh}_3\text{-5Rh}(\text{CO})/\text{SBA-15}$.

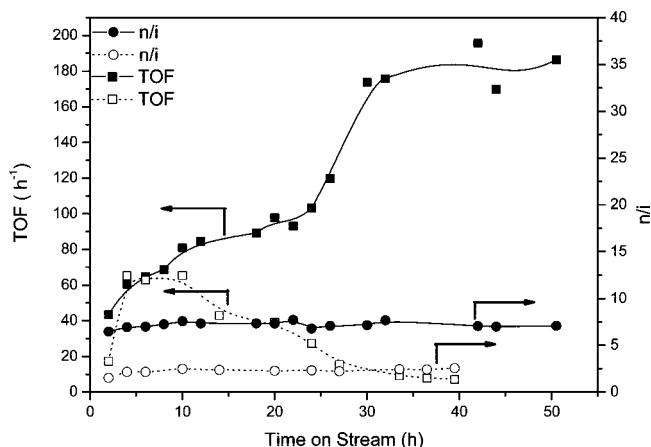


Figure 6. TOFs and n/i ratios of butyraldehyde on $\text{PPh}_3\text{-1Rh}(\text{CO})/\text{SBA-15}$ (the solid line) and $\text{HRh}(\text{CO})(\text{PPh}_3)_3/\text{SBA-15}$ (the dotted line) catalysts (reaction pressure, 1.0 MPa; SV of propene, 500 h^{-1} ; temperature, 403 K).

dispersion (~ 0.51) into account, although the Rh content is nearly the same as that in the supported Wilkinson complex $\text{HRh}(\text{CO})(\text{PPh}_3)_3/\text{SBA-15}$ catalyst.

4. Conclusions

As demonstrated by XRD and N_2 adsorption, Rh complexes can be included in the mesochannels of SBA-15. Quantitative ^1H and ^{29}Si MAS NMR show that the silanol hydroxyls on the surface of SBA-15 can react with rhodium carbonyls to form Si-O-Rh species. Such species are further confirmed by the two-dimensional ^{17}O MQ MAS NMR experiments. Thus, the $\text{PPh}_3\text{-Rh}(\text{CO})$ complex can be tightly grafted on the SBA-15 support through the Si-O-Rh bonds at the interface between the catalyst and the support. ^{31}P MAS NMR spectra reveal that the similar Wilkinson complex structure is formed in the heterogeneous $\text{PPh}_3\text{-Rh}(\text{CO})/\text{SBA-15}$ catalyst. The formation of Si-O-Rh bonds at the interface between the catalyst and the support may immobilize the rhodium complex during the reaction. These may be correlated to the higher activity and stability of heterogeneous $\text{PPh}_3\text{-Rh}(\text{CO})/\text{SBA-15}$ catalyst in propene hydroformylation than those in the supported Wilkinson complex $\text{HRh}(\text{CO})(\text{PPh}_3)_3/\text{SBA-15}$ catalyst.

Acknowledgment. We thank Prof. C. P. Grey and Dr. L. Peng of the State University of New York at Stony Brook for the preparation of the ^{17}O -enriched SBA-15 and help with the ^{17}O MQ MAS NMR experiments. We are also grateful for the financial support of the National Natural Science Foundation of China (No. 20673111, 20573106, 20873140) and the Ministry of Science and Technology of China through the National Key Project of Fundamental Research (No. 2009CB623507). We also thank Prof. R. Prins of ETH Zurich for the fruitful discussion and suggestions.

Supporting Information Available: One-dimensional ^{17}O MAS NMR spectra of all the samples. This material is available free of charge via the Internet at <http://pubs.acs.org>.

References and Notes

- Roelen, O. U.S. Patent 2327066, 1943.
- van Leeuwen, P. W. N. M.; Claver, C., Eds. *Rhodium Catalyzed Hydroformylation*; Kluwer Academic: Dordrecht, 2000; p 6.
- Beller, M.; Cornils, B.; Frohning, C. D.; Kohlpaintner, C. W. *J. Mol. Catal. A* **1995**, *104*, 17.
- Herrmann, W. A.; Cornils, B. *Angew. Chem., Int. Ed.* **1997**, *36*, 1048.
- Zheng, X. L.; Jiang, J. Y.; Liu, X. Z.; Jin, Z. L. *Catal. Today* **1998**, *44*, 175.
- Meehan, N. J.; Sandee, A. J.; Reek, J. N. H.; Kamer, P. C. J.; van Leeuwen, P. W. N. M.; Poliakov, M. *Chem. Commun.* **2000**, 1497.
- (a) Chauvin, Y.; Musmann, L.; Oliver, H. *Angew. Chem., Int. Ed.* **1996**, *34*, 2698. (b) Haumann, M.; Dentler, K.; Joni, J.; Riisager, A.; Wasserscheid, P. *Adv. Syn. Catal.* **2007**, *349*, 425.
- De Munck, N. A.; Verbruggen, M. W.; De Leur, J. E.; Scholten, J. J. F. *J. Mol. Catal.* **1981**, *11*, 331.
- Arhancet, J. P.; Davis, M. E.; Merola, J. S.; Hanson, B. E. *Nature (London)* **1989**, *339*, 454.
- (a) Asakura, K.; Kitamura-Bando, K.; Isobe, K.; Arakawa, H.; Iwasawa, Y. *J. Am. Chem. Soc.* **1990**, *112*, 3242. (b) Asakura, K.; Kitamura-Bando, K.; Iwasawa, Y.; Arakawa, H.; Isobe, K. *J. Am. Chem. Soc.* **1990**, *112*, 9096.
- Mukhopadhyay, K.; Chaudhari, R. V. *J. Catal.* **2003**, *213*, 73.
- Yan, L.; Ding, Y. J.; Zhu, H. J.; Xiong, J. M.; Wang, T.; Pan, Z. D.; Lin, L. W. *J. Mol. Catal. A* **2005**, *234*, 1.
- Klinowski, J. *Chem. Rev.* **1991**, *91*, 1459.
- Amoureux, J. P.; Bauer, F.; Ernst, H.; Fernandez, C.; Freude, D.; Michel, D.; Pingel, U. T. *Chem. Phys. Lett.* **1998**, *285*, 10.
- Peng, L.; Huo, H.; Liu, Y.; Grey, C. P. *J. Am. Chem. Soc.* **2007**, *129*, 335.
- Frydman, L.; Harwood, J. S. *J. Am. Chem. Soc.* **1995**, *117*, 5367.
- Evans, D.; Osborn, J. A.; Wilkinson, G. J. *J. Chem. Soc. A* **1968**, 3133.
- Zhang, W. P.; Sun, M. Y.; Prins, R. *J. Phys. Chem. B* **2003**, *107*, 10977.
- Massiot, D.; Fayon, F.; Capron, M.; King, I.; LeCalvé, S.; Alonso, B.; Durand, J. O.; Bujoli, B.; Gan, Z.; Hoatson, G. *Magn. Reson. Chem.* **2002**, *40*, 70.
- Zhao, P.; Neuhoff, P. S.; Stebbins, J. F. *Chem. Phys. Lett.* **2001**, *344*, 325.
- van Bokhoven, J. A.; Koningsberger, D. C.; Kunkeler, P.; Kentgens, A. P. M. *J. Am. Chem. Soc.* **2000**, *122*, 12842.
- Marler, B.; Oberhagemann, U.; Vortmann, S.; Gies, H. *Microporous Mater.* **1996**, *6*, 375.
- Zhang, W. P.; Ratcliffe, C. I.; Moudrakovski, I. L.; Tse, J. S.; Mou, C. Y.; Ripmeester, J. A. *Microporous Mesoporous Mater.* **2005**, *79*, 195.
- Hunger, M. *Catal. Rev.-Sci. Eng.* **1997**, *39*, 345.
- Xu, X.; Gerstein, B. C.; King, T. S. *J. Catal.* **1989**, *118*, 238.
- Duckett, S. B.; Newell, C. L.; Eisenberg, R. *J. Am. Chem. Soc.* **1994**, *116*, 10548.
- Bianchini, C.; Lee, H. M.; Meli, A.; Vizza, F. *Organometallics* **2000**, *19*, 849.
- Epping, J. D.; Chmelka, B. F. *Curr. Opin. Colloid Interface Sci.* **2006**, *11*, 81.
- Engelhardt, G.; Michel, D. *High-Resolution Solid-State NMR of Silicates and Zeolites*; Wiley: New York, 1987; p 97.
- Dirken, P. J.; Smith, M. E.; Whitfield, H. J. *J. Mater. Chem.* **1995**, *99*, 395.
- Lee, S. L.; Stebbins, J. F. *Am. Mineral.* **2003**, *88*, 493.
- Dirken, P. J.; Kohn, S. C.; Smith, M. E.; van Eck, E. R. H. *Chem. Phys. Lett.* **1997**, *266*, 568.

(33) Lafuma, A.; Fayon, F.; Massiot, D.; Chodorowski Kimmes, S.; Sanchez, C. *Magn. Reson. Chem.* **2003**, *41*, 944.

(34) Mukhopadhyay, K.; Mandale, A. B.; Chaudhari, R. V. *Chem. Mater.* **2003**, *15*, 1766.

(35) (a) van't Blik, H. F. J.; van Zon, J. B. A. D.; Koningsberger, D. C.; Prins, R. *J. Mol. Catal.* **1984**, *25*, 379. (b) van't Blik, H. F. J.; van Zon,

J. B. A. D.; Huizinga, T.; Vis, J. C.; Koningsberger, D. C.; Prins, R. *J. Am. Chem. Soc.* **1985**, *107*, 3139.

(36) Suzuki, A.; Inada, Y.; Yamaguchi, A.; Chihara, T.; Yuasa, M.; Iwasawa, Y. *Angew. Chem., Int. Ed.* **2003**, *42*, 4795.

JP810432P